Journal of Power Sources 189 (2009) 748–751

Contents lists available at ScienceDirect

Journal of Power Sources

journal homepage: www.elsevier.com/locate/jpowsour

Short communication

Lithium metal phosphates, power and automotive applications

H. Huang, T. Faulkner*, J. Barker, M.Y. Saidi

Valence Technology Inc., 1889 E. Maule Ave., Las Vegas, NV 89119 USA

ARTICLE INFO

Article history:
Received 26 June 2008
Received in revised form 4 August 2008
Accepted 6 August 2008
Available online 22 August 2008

Keywords:
Lithium ion
Phosphate
Vanadium
Intercalation

ABSTRACT

Lithium metal phosphate materials are the newest generation of active materials. With the limited number of cathode materials available at present and the prevalence of transition metal oxide cathodes, phosphates are able to answer the rising safety concerns surrounding the oxide chemistry. These inherent safety limitations have until now prevented lithium ion batteries in general from entering the large format applications markets such as electric and hybrid electric vehicles. Iron-based olivine phosphate has been the focus of extensive research: intrinsic thermal stability and continual improvement of its performance characteristics have geared the industry to a fast track adoption of this chemistry for the larger format applications. Recently developed vanadium-based phosphates possess operating voltages of 3.65 V for $Li_3V_2(PO_4)_3$ and 4.05 V for $LiVPO_4F$, both of which are higher than the iron-based phosphate. The high power capability of $Li_3V_2(PO_4)_3$ makes it ideal for applications that require power; $LiVPO_4F$ on the other hand has high energy and a desirable cycling characteristic that makes it ideal for energy-demanding applications such as PHEV and EV. These materials are the best fit for the ever-increasing demand for energy, power and thermal stability that is essential in the large format arena.

1. Introduction

With the aggressive demand for more power to satisfy emerging markets such as power tools, and particularly, the rapidly growing automotive segment, focus is being directed at the lithium ion battery to play the dominant role. With energy densities exceeding 130 Wh Kg^{-1} and cycle life of more than 1000 cycles, the lithium ion chemistry stands to be the chemistry of choice. However, compared with traditional markets like laptops and cellular phones, new applications have much higher energy and power requirements. In these large format applications, where safety is of paramount importance, the use of $LiCoO_2$ and its derivatives raises serious concerns for developers because of inherent thermal instability. Alternatively, lithium metal phosphates have now been widely recognized as a new generation of materials that can offer the safety, power and energy to satisfy these fast growing large platform applications.

The coordinating ability and size of the phosphate anion enables a wide variety of structures, many with ion-conducting channels ideal for lithium conduction. Phosphate structures that have been used or considered for use as lithium ion cathode materials include olivine $LiFePO_4$ [1–12] and the subjects of this paper: nasicon-based $Li_3V_2(PO_4)_3$ [13–20] and triclinic $LiVPO_4F$ [21–23]. Because the oxygen–phosphorus bond in a phosphate material is largely covalent in nature and stronger than a polar oxygen–metal bond, phosphate cathodes have superior thermal stability and a larger inductive effect. These cathodes tend to use redox couples with lower valency than the oxides, which require reducing conditions to synthesize. The proprietary carbothermal reduction (CTR) method developed by Valence Technology [4,24,25] has proven to be a particularly efficient and economical way to synthesize low-valent materials such as the lithium iron phospho-olivine. It also works well for the vanadium-based phosphates, such as $Li_3V_2(PO_4)_3$ and $LiVPO_4F$. In this paper we will present our recent work on these vanadium-based phosphate and fluorophosphate materials.

2. Experimental

2.1. Material syntheses

All starting compounds were weighed out in a ratio with the same stoichiometry as the final product; carbon black was added as both a conductive and a reducing agent. This mixture was suspended in acetone and ball milled. After evaporating the solvent, the resulting mixtures were pelletized and then heated under a flowing Argon atmosphere.

Monoclinic $Li_3V_2(PO_4)_3$, was prepared from V_2O_5 (Alfa Aesar, 99.2%), LiH_2PO_4 (Aldrich 99%) and carbon (Super P) mixed in a molar ratio of 1:3:3; the carbon both reduces pentavalent vanadium to the trivalent state and leaves behind several percent residual

* Corresponding author. Tel.: +1 702 558 1051; fax: +1 702 558 1001.
E-mail address: titus.faulkner@valence.com (T. Faulkner).

0378-7753/$ – see front matter © 2008 Elsevier B.V. All rights reserved.
doi:10.1016/j.jpowsour.2008.08.024

carbon after calcination. The mixture was heated at a temperature of 900 °C for 8 h. $LiVPO_4F$ was prepared via a two-step route involving VPO_4 and LiF. The reaction scheme is outlined below:

$$V_2O_5 + 2(NH_4)_2HPO_4 + 2C \rightarrow 2VPO_4 + 4NH_3 + 3H_2O + 2CO \quad (1)$$

$$VPO_4 + LiF \rightarrow LiVPO_4F \quad (2)$$

The precursors were intimately mixed by ball milling and then pelletized for each separate step in the reaction. To ensure complete reduction of the vanadium from pentavalent to trivalent, 50% excess carbon was added above the stoichiometric amount implicit in reaction (1). Precursor mixture for reaction (1) was slowly heated to a temperature between 600 °C and 700 °C and held at that temperature for a period of 4 h; precursor mixture for reaction (2) was heated to 700 °C and held at that temperature for 1 h.

The fundamental electrochemical properties of the as-prepared materials were characterized using lithium half-cells. Electrodes were prepared by mixing active material, Super P carbon and polyvinylidene fluoride copolymer (Kynar 2801, ARKEMA), where the amount of carbon in the electrode consisted of partly the residual from synthesis and a part that was added during the electrode formulation. These components were mixed in acetone, and the resulting slurry was coated onto aluminum foil. After the acetone evaporated, electrodes were pressed and punched into a disc with an active area of 2.85 cm^2 with an active loading of ~12 mg cm^{-2}. Electrochemical measurements included constant current charge and discharge and electrochemical voltage spectroscopy (EVS).

A prismatic lithium ion cell configuration was chosen to evaluate the power and long-term performance characteristics of the materials. This consisted of a cathode with area of 15 cm^2 and polyethylene separator (Celgard 2300, Celgard LLC). Electrodes were fabricated by mixing active material with Super P and polyvinylidene fluoride (PVdF, KF 7200, Elf Atochem) in *N*-methylpyrrolidone (NMP, 99% Aldrich) solution; the resulting slurry was coated on aluminum foil. The composition of the electrode was 89% active material, 7% carbon and 4% binder. Electrodes were dried at 120 °C under vacuum and then compressed. Graphite anodes were prepared from MCMB (Osaka Gas) with 3% conductive carbon.

3. Results and discussions

3.1. Nasicon-based vanadium phosphate $Li_3V_2(PO_4)_3$

Early work indicated that the performance of the Olivine and Nasicon-based materials was limited by the relatively poor electronic conductivity of the material. Recent investigations have led to improvements in the material utilization by the addition of a conductive carbon layer and by use of preparative approaches that control the product morphology.

$Li_3V_2(PO_4)_3$ is emerging as a very attractive phosphate cathode material [15,16]. Compared with the olivine iron-based phosphate, it offers potentially 40% more energy as shown in Fig. 1. Another attractive property of this phosphate is its intrinsic fast ionic conductivity, critical for applications requiring a high power to energy ratio. To evaluate its ionic conductivity, a prismatic Li ion cell with a Li metal electrode as a reference was constructed. Cathode formulation was 86% active material, 8% carbon and 6% PVDF binder. The cell was first cycled three times at C/5 between 2.5 V and 4.6 V and then fully charged to 4.6 V. The cell was tested using the galvanostatic intermittent titration technique (GITT) regime [29,30]. After charging at 23 °C, the fully charged cell was discharged at I_0 corresponding to a C/25 rate for an interval τ of 1 h followed by an open circuit stand for 5 h to allow cell voltage to relax to its steady-state value, E_s. This procedure was repeated until the cell was fully discharged to 2.5 V. The Li^+ diffusion coefficient D_{Li} was derived from

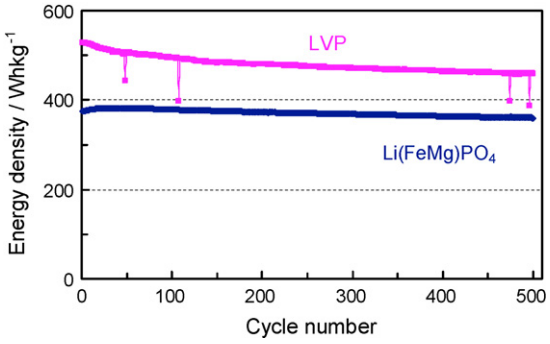

Fig. 1. Energy density retentions with C/2 cycling (23 °C) for lithium ion cells with $Li(FeMg)PO_4$ and $Li_3V_2(PO_4)_3$ cathodes. Energy density calculations are based on the mass of the cathode active materials.

the following relationship [29,30].

$$D_{Li} = \frac{4}{\pi\tau} \times \left(\frac{m_B V_m}{M_B A}\right)^2 \times \left(\frac{\Delta E_s}{\Delta E_\tau}\right)^2$$

The discharge interval time is τ (in this case 1 h); m_B and M_B are, respectively, active mass used and the molecular weight of the compound; V_m is its molar volume; and A is the total contact area between the electrolyte and the electrode. ΔE_s and ΔE_τ are the changes in cathode voltages, the former is the steady-state voltage for a stand time of given duration, in this case 5 h, and the latter is the total transient voltage change for a time duration of discharge interval τ (1 h). V_m is a function of x in $Li_xV_2(PO_4)_3$, and its values at $x = 0, 1, 2$ and 3 have been reported previously [20]. Literature methods for determining parameter A use either the geometric electrode surface area; or an approximation of the actual surface area derived from BET measurements or some other means [30]. In this paper we have chosen to use the geometric surface area of the electrode for this purpose. In Fig. 2, D_{Li} is shown as a function of the discharge capacity. These measurements confirm the fast ionic character of the lithium vanadium phosphate electrode, with values for D_{Li} on the order of 10^{-9} cm s^{-1}, which is among the highest measured for any cathode. This is a very valuable characteristic in fast rate and power applications.

The rate dependent capability of $Li_3V_2(PO_4)_3$ cathode was evaluated in a prismatic Li ion cell at different rates ranging from C/2 up to 20 C and is presented in Fig. 3. Electrode formulation contained 88% active, 8% carbon and 4% PVDF binder. The data include the rate corresponding discharge voltage profiles at C/2, 5 C, 10 C, 15 C and 20 C rates, and the resulting capacity retentions. It is notable that this cathode performs extremely well, and still retains above 80% of its original capacity at rates as high as 20 C. With respect to the smaller prismatic cell format, the heating that normally occurs at

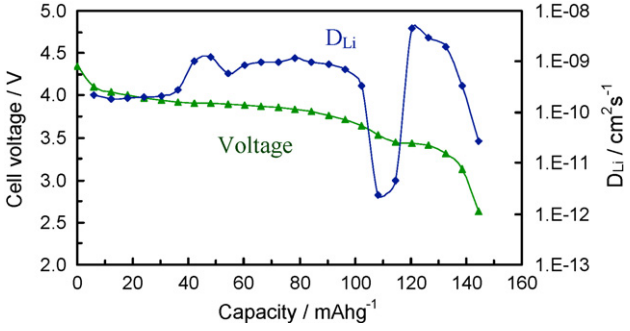

Fig. 2. Variation of D_{Li} as a function of cell capacity for $Li_3V_2(PO_4)_3$.

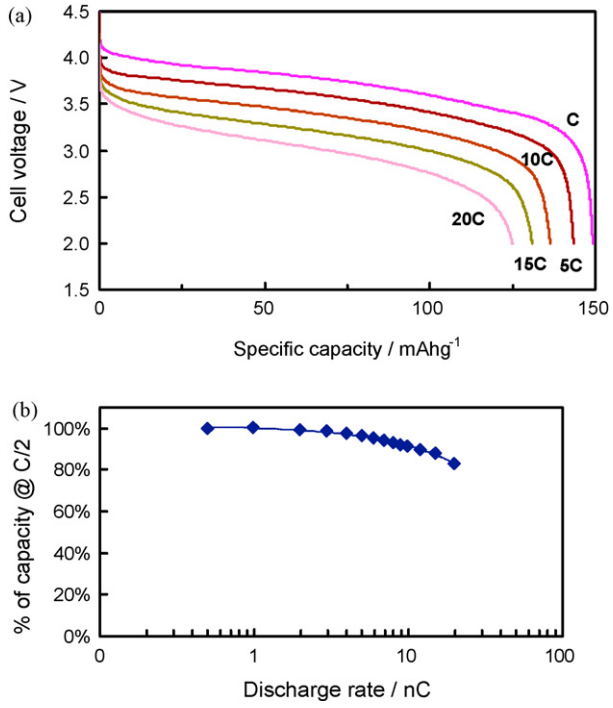

Fig. 3. Discharge voltage profiles (a) and rate capacity retention (b) at different discharge rates for a prismatic Li ion cell with $Li_3V_2(PO_4)_3$ cathode (cathode active loading: 7.5 mg cm^{-2}; rate: C/2; 23 °C).

high discharge rates and greatly assists cell performance is absent. We are herein measuring the true intrinsic capability of the material. With the best rate and power capability among all phosphate materials studied to date, this chemistry promises to be an ideal fit for HEVs and particularly PHEVs.

3.2. Lithium vanadium fluorophosphate: $LiVPO_4F$

The extraction of lithium from $LiVPO_4F$ relies upon the oxidation and reduction of the V^{3+}/V^{4+} couple. Fig. 4(a) shows the EVS first

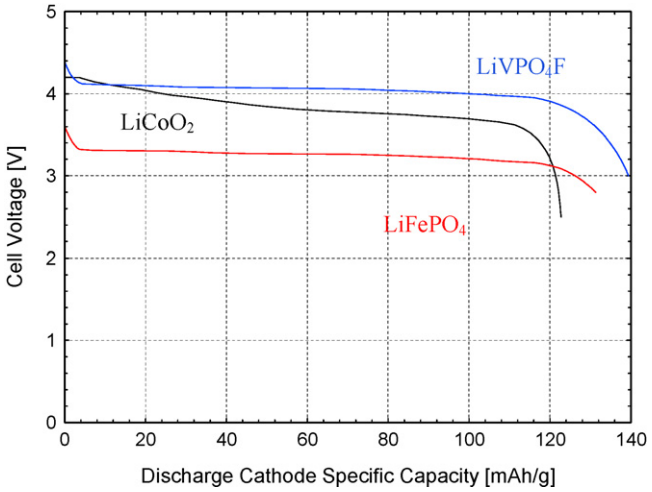

Fig. 5. Comparative voltage profiles for graphite/$LiVPO_4F$, graphite/$LiCoO_2$ and graphite/$LiFe[Mg]PO_4$. The data was collected at an approximate C/8 rate. The electrolyte used in all iterations comprised 1 M $LiPF_6$ in EC:DMC (2:1) by weight.

cycle data for Li/$LiVPO_4F$ cell. The cathode was formulated with 82% LVPF, 8% carbon and 10% PVDF binder. Reversible specific capacity was close to its theoretical value of 155 mAh g^{-1}; the voltage trace also confirmed the system's very low level of polarization. This performance is a significant improvement over our past publications [31,32] and is the result of the improvements realized from optimization of the preparative conditions. Fig. 4(b) depicts the differential capacity plot for the Li/$LiVPO_4F$ system, which reveals the presence of two closely spaced peaks during charge. This in turn is associated with Li extraction from two inequivalent crystallographic sites. In contrast, the discharge step exhibits a single peak consistent with a two-phase behavior. This electrochemical response recorded during the initial EVS cycle persists over several hundred cycles and may be considered characteristic of the lithium insertion reactions.

In Fig. 5, we compare the voltage profiles of graphite//$LiVPO_4F$ and graphite//$LiCoO_2$ using identical anodes with similar loading and mass balance. The reversible specific capacities of the two

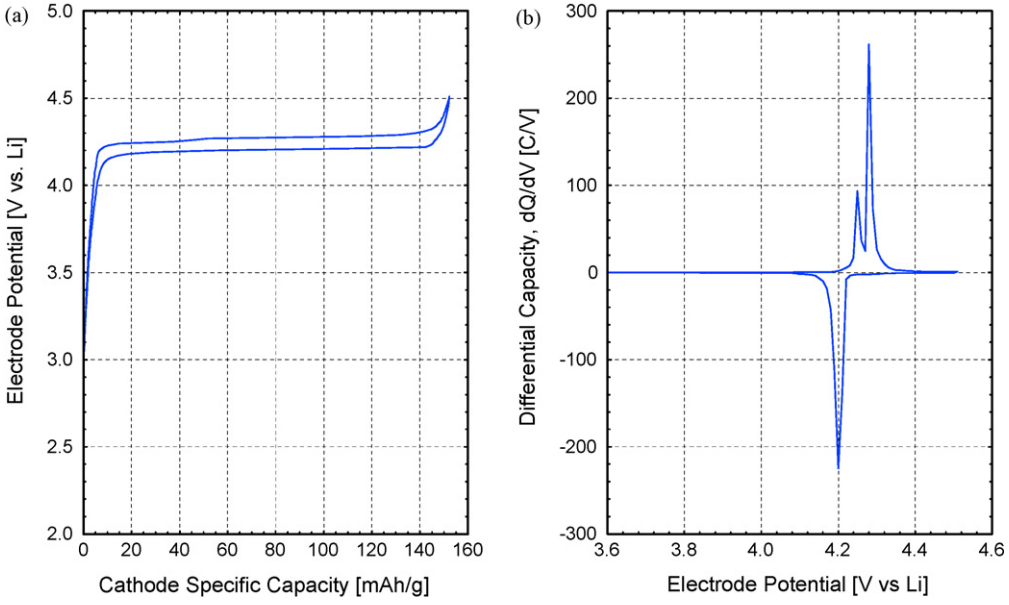

Fig. 4. EVS data for a graphite/$LiVPO_4F$ cell cycled between 3 V and 4.5 V. (a) EVS voltage profile. (b) EVS differential capacity.

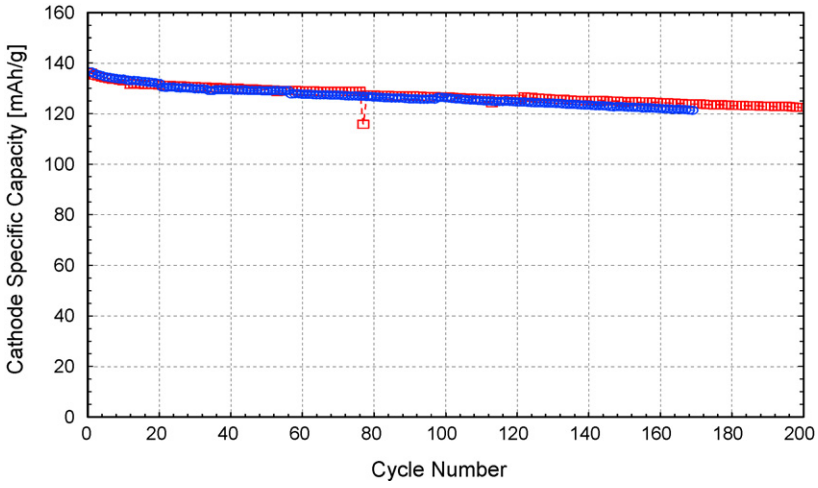

Fig. 6. Lifetime cycling of a graphite/$LiVPO_4F$ lithium ion cell at C/2 rate and 23 C.

active materials were determined to be similar, i.e. 129 mAh g^{-1} and 132 mAh g^{-1} for the $LiVPO_4F$ and $LiCoO_2$, respectively. By comparison, the vanadium fluorophosphate offers not only a flatter voltage profile but also an average voltage that is 0.3 V higher than the comparable $LiCoO_2$ and 0.8 V higher than the iron-based phosphate. In addition to these fundamental differences, safety considerations are of paramount importance in establishing that $LiVPO_4F$ would be a viable alternative to the oxide especially in the large format applications. Based on the similarity of the M–O–P bonding to for example olivine $LiFePO_4$, we would expect $LiVPO_4F$ to offer substantially better safety characteristics than cobalt oxide.

In Fig. 6, we demonstrate the long-term performance of the graphite//$LiVPO_4F$ lithium ion system at a C/2 cycling rate. The cycling performance confirms that the $LiVPO_4F$ system offers good long-term stability with comparatively low fade characteristics. This is comparable to similar lithium ion battery testing using commercial grade $LiCoO_2$.

4. Conclusions

In seeking the goal of higher energy and higher power density for large-format batteries while still maintaining a high degree of safety, phosphate cathodes are the candidates of choice. Olivine $Li(FeMg)PO_4$ has already proven its usefulness in commercial cells; new vanadium-based phosphates hold out the promise of more energy and higher power while still maintaining the phosphate safety edge. The unique properties of $Li_3V_2(PO_4)_3$ in particular are its excellent rate capability and a high operating voltage of 3.65 V: it is a good candidate for applications requiring power capability. The fluorophosphate $LiVPO_4F$ with its combination of a 4.05-V operating voltage and desirable cycling characteristics is a viable contender for high-energy applications in the PHEV and EV markets. For large format and automotive applications where safety is paramount, the intrinsic safety characteristics of both phosphate materials add considerably to their viability.

References

[1] A.K. Padhi, K.S. Nanjundaswamy, J.B. Goodenough, J. Electrochem. Soc. 144 (1997) 1188–1194.
[2] A.K. Padhi, K.S. Nanjundaswamy, C. Masquelier, S. Okada, J.B. Goodenough, J. Electrochem. Soc. 144 (1997) 1609–1613.
[3] J. Barker, M.Y. Saïdi, US Patent 6,884, 544.
[4] J. Barker, M.Y. Saidi, J.L. Swoyer, Electrochem. Solid-State Lett. 6 (2003) A53–A55.
[5] N. Ravet, J.B. Goodenough, S. Besner, M. Simoneau, P, Hovington, M. Armand, Abstract 127, 196th ECS, Honolulu, Hawaii, 1999, 17–22.
[6] N. Ravet, Y. Chouinard, J.F. Magnan, S. Besner, M. Gauthier, M. Armand, J. Power Sources 97/98 (2001) 503.
[7] A. Yamada, S.C. Chung, K. Hinokuma, J. Electrochem. Soc. 148 (2001) A224–A229.
[8] H. Huang, S.-C. Yin, L.F. Nazar, Electrochem. Solid-State Lett. 4 (2001) A170–A172.
[9] S.Y. Chung, J.T. Bloking, Y.M. Chiang, Nat. Mater. 1 (2002) 123–128.
[10] V. Srinivasan, J. Newman, J. Electrochem. Soc. 151 (2004) A1517–A1529.
[11] V. Srinivasan, J. Newman, Electrochem. Solid-State Lett. 9 (2006) A110–A114.
[12] A. Yamada, H. Koizumi, N. Sonoyama, R. Kanno, Electrochem. Solid-State Lett. 8 (2005) A409–A413.
[13] A.K. Padhi, K.S. Nanjundaswamy, C. Masquelier, J.B. Goodenough, J. Electrochem. Soc. 144 (1997) 2581–2586.
[14] J. Barker, M.Y. Saïdi; US Patent 5,871,866 (1999).
[15] M.Y. Saïdi, J. Barker, H. Huang, J.L. Swoyer, G. Adamson, Electrochem. Solid-State Lett. 5 (2002) A149–A151.
[16] M.Y. Saïdi, J. Barker, H. Huang, J.L. Swoyer, G. Adamson, J. Power Sources 119–121 (2003) 266–272.
[17] H. Huang, S.C. Yin, T. Kerr, N. Taylor, L.F. Nazar, Adv. Mater. 14 (2002) 1525–1528.
[18] S.C. Yin, H. Grondey, P. Strobel, H. Huang, L.F. Nazar, J. Am. Chem. Soc. 125 (2003) 326–327.
[19] S.C. Yin, H. Grondey, P. Strobel, M. Anne, L.F. Nazar, J. Am. Chem. Soc. 125 (2003) 10402–10411.
[20] M. Morcrette, J.-B. Leriche, S. Patoux, C. Wurm, C. Masquelier, Electrochem. Solid-State Lett. 6 (2003) A80–A84.
[21] J. Barker, M.Y. Saidi, J.L. Swoyer, J. Electrochem. Soc. 150 (2003) A1394–A1398.
[22] J. Barker, M.Y. Saidi, J.L. Swoyer, J. Electrochem. Soc. 151 (2004) A1670–A1677.
[23] J. Barker, R.K.B. Gover, P. Burns, A. Bryan, M.Y. Saidi, J.L. Swoyer, J. Electrochem. Soc. 152 (2005) A1776–A1779.
[24] J. Barker, M.Y. Saidi, J.L. Swoyer, US Patent 6,528,033.
[25] J. Barker, M.Y. Saidi, J.L. Swoyer, J. Electrochem. Soc. 150 (2003) A684–A688.
[29] W. Weppner, R.A. Huggins, J. Electrochem. Soc. 124 (1977) 1569.
[30] K.M. Shaju, G.V. Subba Rao, B.V.R. Chowdari, J. Electrochem. Soc. 151 (2004) A1324–A1332.
[31] J. Barker, M.Y. Saidi, J. Swoyer, J. Electrochem. Soc., US Patent 6,387,568, issued May 2002.
[32] J. Barker, M.Y. Saidi, J. Swoyer, J. Electrochem. Soc. 150 (2003)A1394.